Disbonding between 2 1/4Cr-1Mo Steel and Overlaid Austenitic Stainless Steel by Means of Electrolytic Hydrogen Charging Technique†

Fukuhisa MATSUDA*, Hiroji NAKAGAWA**, Sanae TSURUTA*** and Yasuyuki YOSHIDA****

Abstract

Disbonding meaning separation-type cracking which occurs at the transition zone between 2 1/4Cr-1Mo steel and overlaid austenitic stainless steel is considered to be attributed to hydrogen accumulation at the transition zone, and has been generally studied with autoclave in laboratory scale. The authors studied to apply electrolytic hydrogen charging technique in the viewpoint of the simplicity of experiment. Main conclusions obtained are as follows:

1) Electrolytic hydrogen charging technique under suitable conditions can be utilized for the purpose of comparative test of disbonding susceptibility.

2) Disbonding easily occurred in PWHT materials overlaid with Type 309, 308, 310. No disbonding occurred in material overlaid with Inconel or Type 309 combined with low carbon 2 1/4Cr-1Mo buttered metal.

3) Microscopic observation showed that the disbonding mainly occurred at the front edge of hardened carbide layer.

KEY WORDS: (Austenitic Stainless Steel) (Heat Resisting Materials) (Hydrogen Embrittlement) (Cracking)

1. Introdution

Investigation on disbonding meaning separation-type cracking which occurs in the vessel of hydro-desulfurizing reactor in oil refining plants operated under hydrogen atomosphere of high temperature and high pressure has been done with autoclave in laboratory scale[1~3]. However, there are yet many indistinct problems concerning the effect of microstructural transistion near weld bond on the disbonding phenomena.

On the other hand, the authors has proved[4] that this type of crack can be simulated utilizing electrolytic hydrogen charging method, which is better than the autoclave method in the viewpoint of the simplicity of experiment. Therefore this method has a possibility to become useful one for the comparative test of disbonding and elucidation of its mechanism, if its testing condition is established.

In the first part, in this study, the optimum condition of the electrolytic hydrogen charging method is studied, and the disbonding susceptibility among different overlaid metals by this method is compared with that by means of the autoclave. Moreover, the relation between microstructural features and the disbonding characteristics is studied.

2. Experimental Procedures

2.1 Materials used

Base metals used were 2 1/4Cr-1Mo steels whose chemical compositions are shown in **Table 1**. Material A is commercially used type 2 1/4Cr-1Mo steel (115 mm thick) and used for overlaying for type 309, 308, 310, 430, Inconel and special low carbon 2 1/4Cr-1Mo filler metals. Material B is overlaid or buttered metal on the material A with the special low carbon 2 1/4Cr-1Mo filler metal and plays the role of the base metal for overlaying with type 309 filler metal. The purpose of base metal B adopted is to investigate the effect of low carbon on disbonding. Material C is used as a base metal (23 mm thick) for diffusion bonding with Type 304. This is to investigate the effect of nil-penetration in boundary zone on disbonding.

Table 1 Chemical compositions of 2 1/4Cr-1Mo base metals and interlayer weld metal buttered.

Material	Chemical composition (wt %)								
	C	Si	Mn	P	S	Ni	Cr	Mo	Nb+Ta
A*	0.13	0.16	0.54	0.005	0.004	–	2.39	1.05	–
B**	0.04	0.31	0.67	0.014	0.006	–	2.63	0.98	0.87
C***	0.12	0.14	0.48	0.009	0.004	–	2.16	0.91	–

* Base metal for overlaying
** Buttered metal for A309BS and P309BS (Buttering condition is shown in Table 2)
*** Base metal for CP in Table 3

† Received on November 1, 1984
* Professor
** Research Instructor
*** Nippon Steel Corp.
**** with Hiroshima Technical Institute, Mitsubishi Heavy Industries, Ltd.

Transactions of JWRI is published by Welding Research Institute of Osaka University, Ibaraki, Osaka 567, Japan

Ten different types of overlaid metals were made on the base metal A or B by combining different type of filler metals and welding conditions in submerged-arc strip-cladding process. Types of filler metals, welding conditions and the designations of the overlaid metals are shown in **Table 2**. The marks S and H in the designation

Table 2 Filler metal and overlaying conditions used in submerged-arc strip cladding process.

Base metal	Filler metal	Size	Overlaying condition** Welding current (A)	Arc voltage (V)	Welding speed (cm/min)	Layer	Designation As-weld	P.W.H.T. 690°Cx26hr
A	Type 309	75x0.4	1200	27	15	2 layer welding	A309S	P309S
		75x0.6	2300	27	40		A309H	P309H
	Type 308	75x0.4	1200	27	15		A308S	P308S
		75x0.4	2300	27	40		A308H	P308H
	Type 310	50x0.4	800	27	15		A310S	P310S
		50x0.4	1500	27	40		A310H	P310H
	Type Inconel	50x0.4	800	27	15		AIncoS	PIncoS
		50x0.4	1500	27	40		AIncoH	PIncoH
	Type 430	50x0.4	800	27	15	1 layer welding	A430S	P430S
B	Buttering* metal	75x0.4	1200	25	15	1 layer welding	A309BS	P309BS
	Type 309		1200	27	15	2 layer welding		

* Low Carbon-2¼Cr-1Mo weld metal
** Preheating and interpass welding temperature:100-150 c

mean standard welding condition (slow speed-low current) and high speed-high current welding condition, respectively. The reason for the use of high speed-high current welding condition is to confirm beneficial effect of large dilution by this condition on disbonding. The mark B in the designation means that buttering of low carbon 2 1/4Cr-1Mo steel was made prior to overlay of Type 309. Furthermore ferritic stainless steel (Designation 430S) was overlaid for the comparison.

The head marks A and P in the designation mean as-welded material and PWHT material, respectively. Therefore, P309S, for example, means the specimen overlaid with Type 309 and PWHT-treated in 690°C x 26hrs after welding.

Also, the diffusion-bonded material which was made with the condition shown in **Table 3** was used.

Table 3 Diffusion bonding conditions of Type 304.

Temperature (°C)	Pressure (kg/cm²) X Holding time (hr)	Degree of vacuum (torr)	P.W.H.T. condition (°c x hr)	Designation
1000	2 X 1, then 0 X 1	10^{-4}	690 X 26	C P

Table 4 shows the chemical compositions at first layer of stainless steel overlaid metals and the diffusion clad metal (CP), together with calculated value of $Ni_{eq.}$ and $Cr_{eq.}$ by Schaeffler diagram.

2.2 Cracking test by electrolytic hydrogen charging method

Hydrogen was charged electrolytically to the specimen. Electrolyte used was aqeous solution of 5% sulfuric acid,

Table 4 Chemical compositions of stainless steel overlaid weld metal at first layer and clad metal.

Material	Chemical composition (wt %) C	Si	Mn	Ni	Cr	Mo	Nb	Nieq	Creq
309S	0.050	0.58	1.40	9.40	19.51	0.24	-	11.60	20.62
309H	0.051	0.33	1.22	7.33	16.00	0.41	-	9.47	16.91
308S	0.035	0.57	1.38	9.06	18.10	0.18	-	10.11	19.14
308H	0.041	0.38	1.30	6.96	15.70	0.38	-	8.84	16.65
310S	0.034	0.27	3.81	18.14	19.46	2.12	-	21.07	21.99
310H	0.053	0.22	3.09	14.14	15.97	1.89	-	17.28	18.19
IncoS	0.030	0.23	2.96	62.99	16.21	0.20	1.80	65.37	17.66
IncoH	0.036	0.20	2.75	58.02	15.36	0.28	1.77	60.48	16.83
430S	0.042	0.81	0.48	0.16	13.30	0.15	-	1.50	14.66
309BS	0.043	0.61	1.38	9.30	19.39	0.23	0.11	11.28	20.59
C P	0.070	0.61	1.24	8.68	18.24	-	-	11.40	19.16

Nieq= Ni+0.5Mn+30C+30N% Creq= Cr+Mo+1.5Si+0.5Nb%

to which phosphorus was added. Platinum was used for the anode. The charging was done in room temperature.

Specimen for cracking test was machined to the configuration shown in **Fig. 1(a)**, where the thickness of base metal is an important factor in this test, and is described later. **Figure 1(b)** shows the setting situation of the specimen in the electrolyte. Other surfaces except for the bottom surface were insulated with sticky tapes. The depth soaked in the electrolyte was about 2 mm. No load was applied in this test. In this test hydrogen accumulation and thus disbonding was expected to occur at the

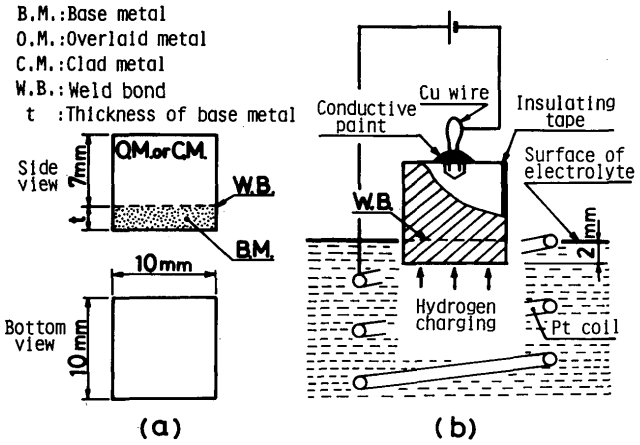

Fig. 1 (a) Shape of specimen for cracking test, and (b) setting situation of the specimen in the electrolyte

transition zone in overlaid austenitic weld metal because of the higher solubility and the lower diffusibility in the austenitic structure. The cracking test was composed of the next three series:

Exp. 1: The concentration of hydrogen near the weld bond was considered to be affected by the thickness of base metal, because hydrogen was charged from the bottom surface of base metal. Also, the escape of hydrogen from the side surfaces was considered to depend on the thickness of base metal. Therefore, the optimum

thickness was studied for the material CP and P309S.

Exp. 2: In order to study the effect of current density and charging time on disbonding, the cracking test was done under various condition for materials P309S and P310S. In this experiment, 2 mm thickness of base metal was selected on the basis of the result in Exp. 1.

Exp. 3: Disbonding susceptibility among different overlaid materials were compared on the basis of Exps. 1 and 2.

After the hydrogen charging, the specimen was left in the air for more than 24hr, and then was cut perpendicularly to the weld bond at the middle section. Crack was checked with optical microscope in the magnification of 400. Crack ratio was defined as follows: As shown in **Fig. 2**, 21 lines perpendicular to the weld bond were drawn, and the number of intersections with cracks was counted. Now the crack ratio was calculated as the ratio of intersecting number to total lines (21). Also the distance of crack from the weld bond (d) and width of carbide layer (w) was defined as shown in Fig. 2.

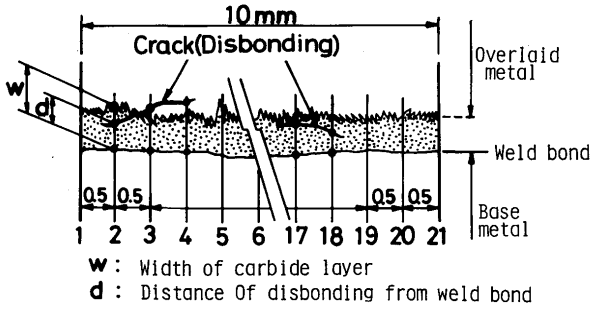

Fig. 2 Definition of crack ratio, distance of crack from bond and width of carbide layer

2.3 Measurement of hardness and observation of microstructure and fracture surface

The distribution of hardness was measured with micro-Vickers hardness tester. Load used was 10gf because variation of hardness at near the weld bond was very steep.

Observation of microstructure and fracture surface was done with optical microscope and scanning electron microscope, respectively. Aquaregia was used for etching.

3. Experimental Results and Discussion

3.1 Results of cracking test with electrolytic hydrogen charging method.

3.1.1 Effect of thickness of base metal on disbonding

Table 5 shows the relation between the thickness of base metal and disbonding, and means that the decrease in the thickness promotes the disbonding. It is noteworthy that the disbonding has a tendency to occur at the center of the specimen width. Microscopically, all these disbondings occurred at the transition zone near the weld bond in the overlaid metal.

Table 5 Effect of base metal thickness on disbonding.

Material	Thickness of base metal t (mm)			
	0.5	2	4	8
P309S	——	7.6 B.M.	3.3 B.M.	No disbonding
CP	9.2 mm Crack B.M.	5.8 B.M.	No disbonding	No disbonding

Hydrogen charging condition
Current density : 0.2A/cm²
Charging time : 24hr

Table 5 suggests that the base metal should be cut as thin as possible. However, the weld bond by submerged-arc process was not so straight, and thus the reproducibility of the thickness less than 2 mm was not satisfactory. Thus the authors decided to utilize 2 mm thickness.

Besides, the result in Table 5 intimates that residual stress has little effect on the disbonding, because the residual stress near the weld bond originated due to the difference in thermal expansion is generally decreased with the reduction in thickness as well known.

3.1.2 Effects of current density and charging time on disbonding

Figure 3 shows the effects of current density and charging time on the disbonding in P309S and P310S, where "Serious disbonding" means the total crack length longer than the half length of the weld bond and "Slight disbonding" means that shorter than the half length. It is seen that high current density and long charging time promote the disbonding, and that P309S is more susceptible than P310S comparing the critical curves. On the basis of this result, the charging condition of 0.2A/cm² and

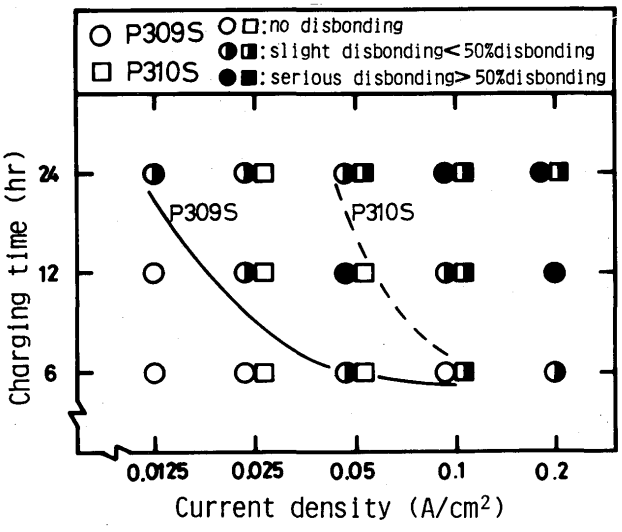

Fig. 3 Effects of current density and charging time on disbonding

24hr was generally selected. The diffusible hydrogen content under this charging condition was 3*ml* per 100g of the specimen shown in Fig. 1(a), which was collected for 48hr at 45°C and measurred by means of gaschromatography.

Generally speaking, the current density gives the hydrogen concentration at the charged surface, and the charging time gives the time for diffusion and accumulation. Therefore the increase in these two variables increase the accumulated hydrogen concentration in overlaid metal near the weld bond. It maybe reasonable that the crack occurs when the accumulated concentration exceeds a certain limit depending on material.

3.1.3. Comparison of disbonding tendency among different overlaid materials

Table 6 summarizes the result of the cracking test by electrolytic charging method together with some results by means of autoclave[5]. As-welded materials were generally very insusceptible to the disbonding except for A309BS which showed tiny cracks in only very severe condition. Comparison of the results between electrolytic and autoclave methods means that the electrolytic condition of 0.2A/cm^2 and 24hr well corresponds to the autoclave condition of 450°C and 220 kgf/cm^2.

In the results by electrolytic charging method, PIncoS, PIncoH and P309BS where low carbon 2 1/4Cr-1Mo material was buttered showed no disbonding, but interestingly P430S which was ferritic stainless overlaid material showed disbonding in the most severe condition.

Besides, blisters were observed in the all charging conditions for the as-welded material, and only in the condition of 0.4A/cm^2 and 48hr for the PWHT materials. The blisters were formed in the base metal, and their location was limited within about 0.5mm from the charging surface. Therefore, it is considered that the blister has no relation to the disbonding.

Table 6 Results of the cracking test by electrolytic charging method together with some results by means of autoclave.

	Material	Electrolytic method: Condition (A/cm^{2}xhr) 0.2x24	0.4x24	0.4x48	Autoclave method: Condition (°cxkg/cm^2) 420x120	450x150	450x220
P.W.H.T.	P309S	●	—	—	○	●	●
	P309H	◑	—	—	○	○	●
	P308S	●	—	—	—	—	—
	P308H	◑	—	—			
	P310S	◑	—	—	○	●	●
	P310H	●	—	—	—	—	—
	PIncoS	○	○	○	○	○	—
	PIncoH	○	○	○	—	—	—
	P430S	○	○	●	—	—	—
	P309BS	○	○	○	○	○	○
	CP	●	—	—	—	●	●
As-weld	A309S	○	○	○			
	A309H	○	○	○			
	A308S	○	○	○			
	A308H	○	○	○			
	A310S	○	○	○			
	A310H	○	○	○			
	AIncoS	○	○	○			
	AIncoH	○	○	○			
	A430S	○	○	○			
	A309BS	○	○	◑			

Electrolytically tested specimen
PWHT:690°cx26hr
Base metal thickness of specimen:2mm
○:No disbonding
◑:Slight disbonding
●:Serious disbonding

Autoclave specimen
PWHT:691°cx24hr
Cooling rate:200°c/hr
○:No disbonding
●:Disbonding

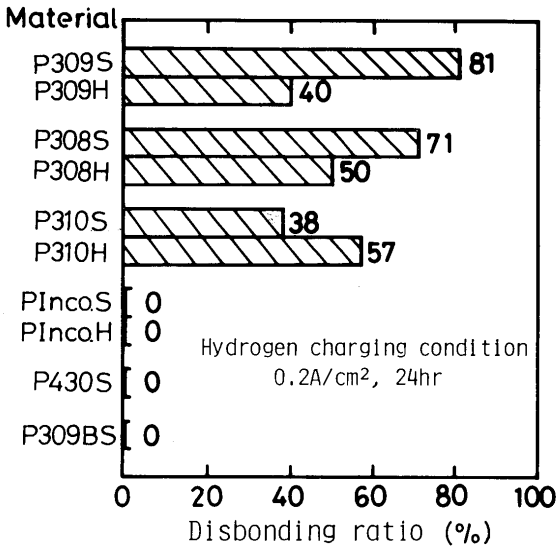

Fig. 4 Disbonding ratio of overlaid material under the conditions of 0.2A/cm^2 and 24hr

Figure 4 gives the disbonding ratio defined in Fig. 2 under the condition of 0.2A/cm^2 and 24hr. Comparison among the standard welding condition (mark S) shows that the disbonding ratio decreases in the order of P309S, P308S and P310S. Comparison between standard welding condition and high current-high speed welding condition (mark H) shows that high current-high speed welding is effective to decrease the crack ratio for types 309 and 308 as reported, but not satisfactory. Interestingly, high current-high speed welding promotes the crack for type 310.

3.2 Relation between microstructure near weld bond and disbonding

3.2.1 Characteristics of microstructure near the weld bond, disbonding and fracture surface

Photograph 1 show the microstructure and disbonding of the each material.

The microstructure in the overlaid weld metal near the weld bond was mainly austenite with sporadic δ-ferrite in 309S, 308S and 309BS in both as welded and PWHT condition, and was mixed structure of austenite and martensite with rare δ-ferrite in 309H and 308H, and mostly

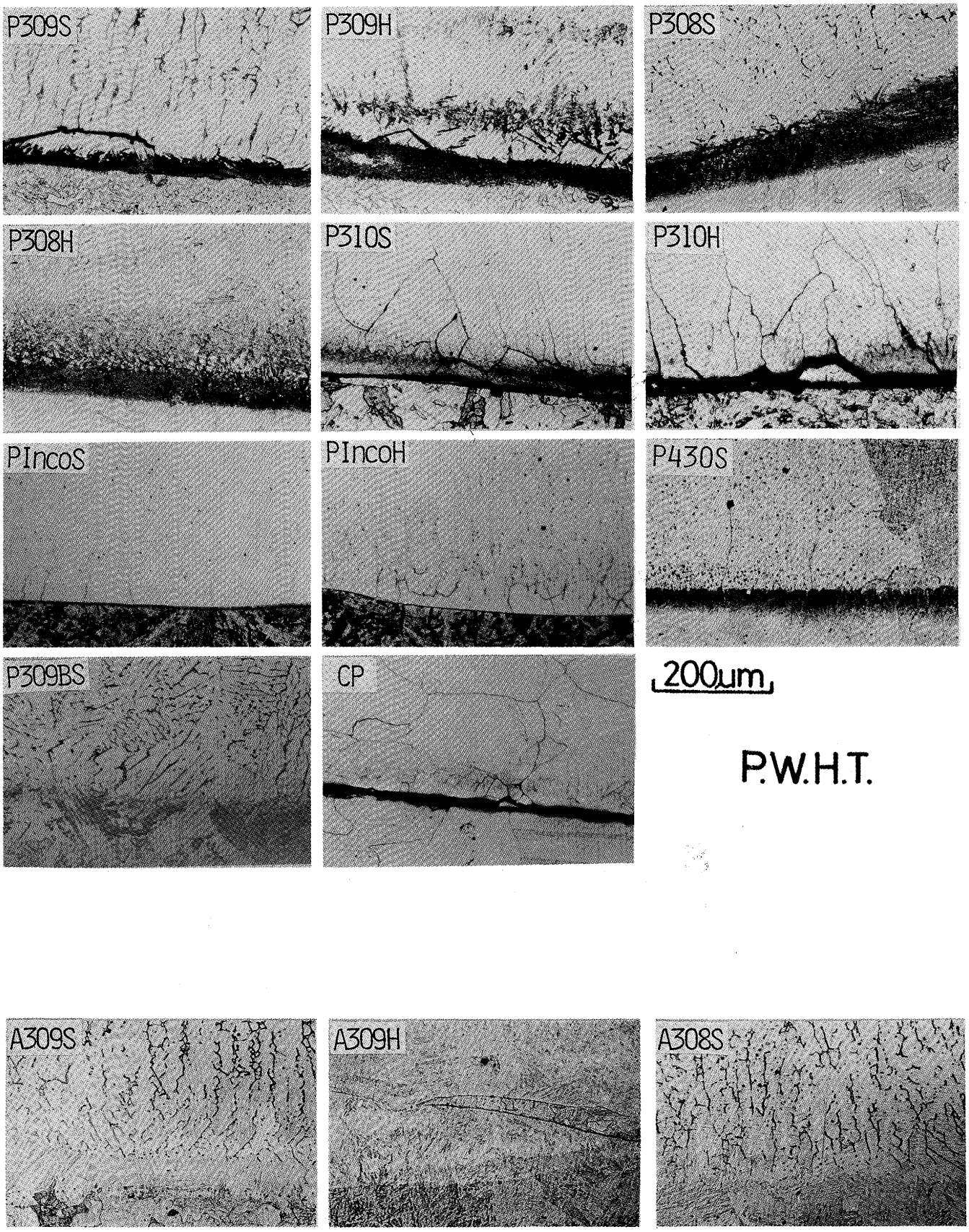

Photo. 1 Typical examples of microstructure and disbonding which occurred under the conditions of 0.2A/cm^2 and 24hr

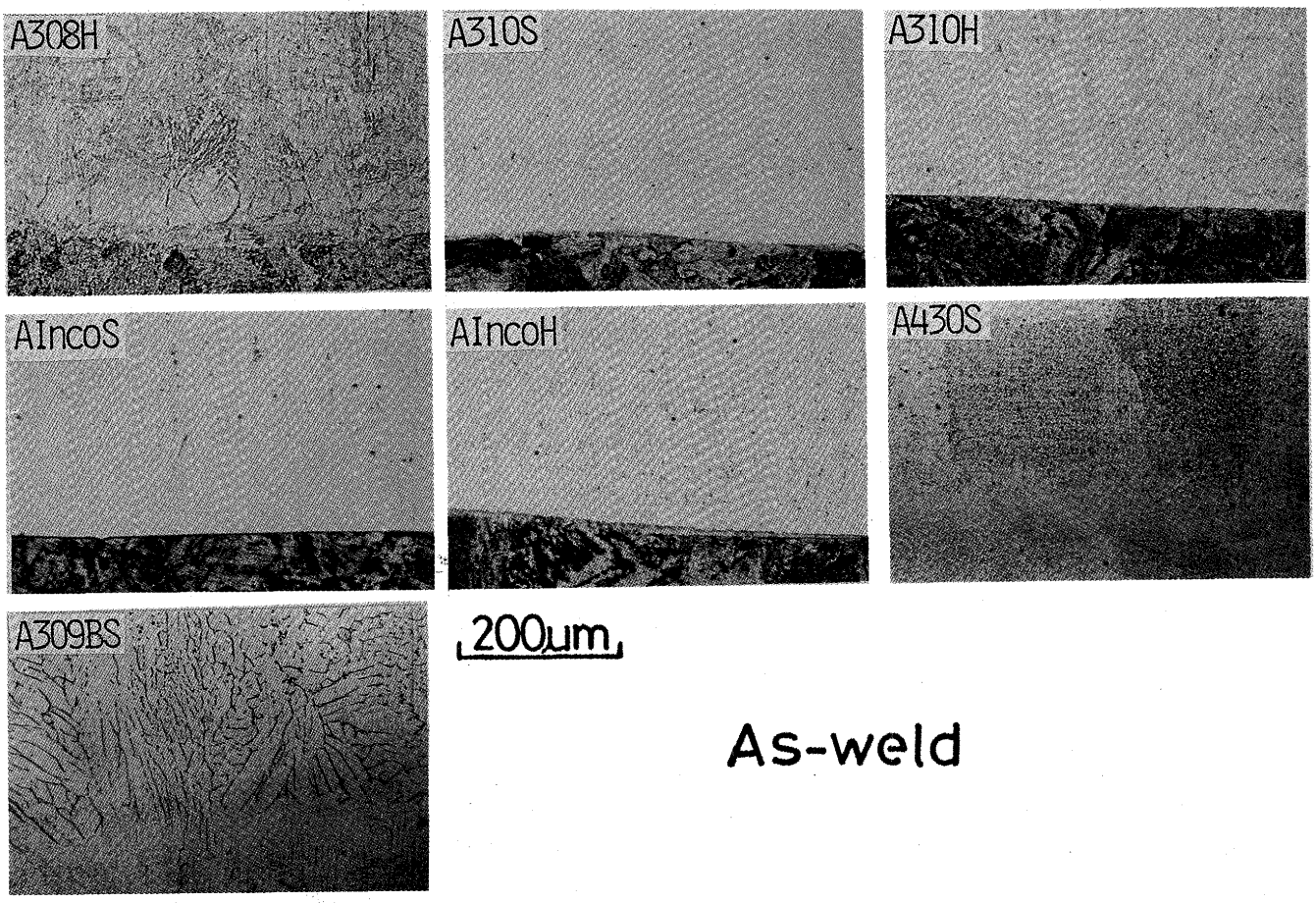

Photo. 1 Continued

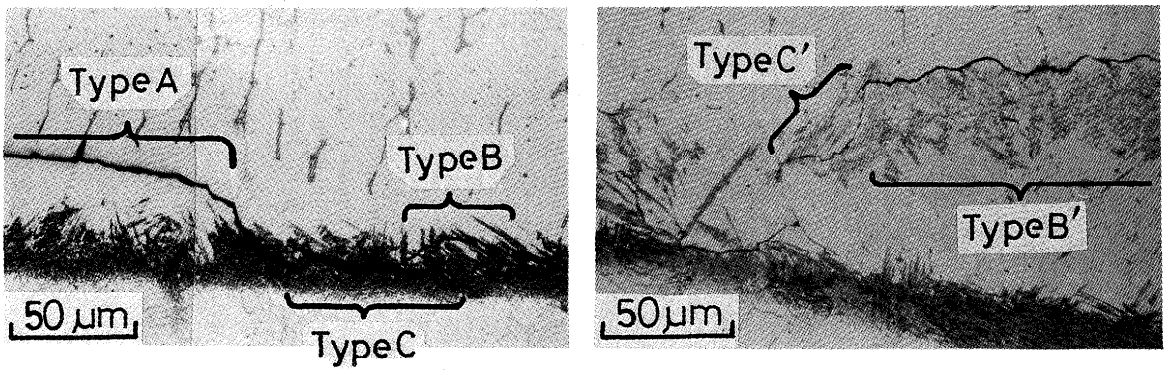

Photo. 2 Five types of disbonding location under the condition of 0.2A/cm² and 24hr

only austenite in 310S, 310H, IncoS and IncoH, and mostly ferrite in 430S.

Extremely near the weld bond lath-like martensite was generally seen, where also carbides maybe precipitate partly. In PWHT material, however, carbide precipitation zone was remarkable as black zone. Moreover coarse austenite grain boundary was clearly seen in PWHT material. In P309BS, carbide precipitation zone was not so clear in spite of PWHT because of buttering of low carbon 2 1/4Cr-1Mo material.

Disbonding location occurred under the condition of 0.2A/cm² and 24hr was classified into five types, namely Types A, B, C, B′ and C′, as shown in **photo. 2(a) and (b)**. (Types A, B and C are nearly the same as those in ref. 4.) Types B′ and C′ were observed only in P309H made by high current-high speed welding. Type B′ occurred along the sawtoothed border between the austenite and the isolated martensite region from weld boundary. Type C′ occurred inside the isolated martensite region.

As seen in Table 6, disbonding occurred even in ferritic stainless overlaid metal under very severe charging condition. **Photograph 3** shows the microstructure around the

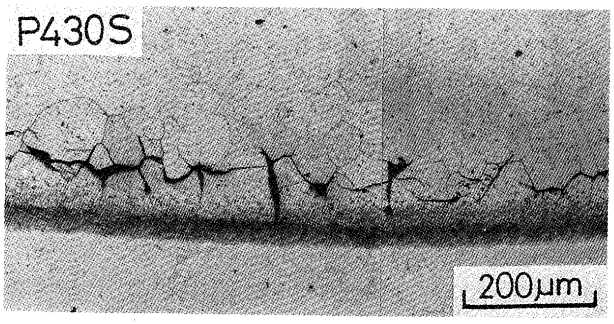

Photo. 3 Microstructure and the disbonding in ferritic stainless overlaid material which occurred under the conditions of 0.4A/cm^2 and 48hr

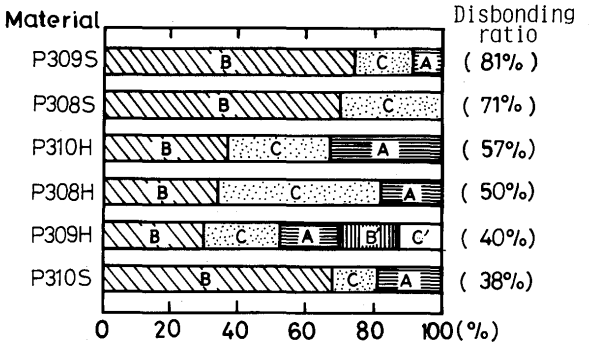

Fig. 5 Percentage of type of disbonding location occurred under the conditions of 0.2A/cm^2 and 24hr

disbonding, which occured as Type A-like, but in mainly transgranular and partly intergranular mode.

Figure 5 shows the percentage of each type, from which it is understood that Type B was the majority in the material of high disbonding ratio. In the material of low disbonding ratio, however, Type A was relatively noticeable a little, although the sum of Types B and C was more than half in any specimen. Thus it is considered that borderning grain boundary to carbide zone or carbide zone itself was susceptible to disbonding.

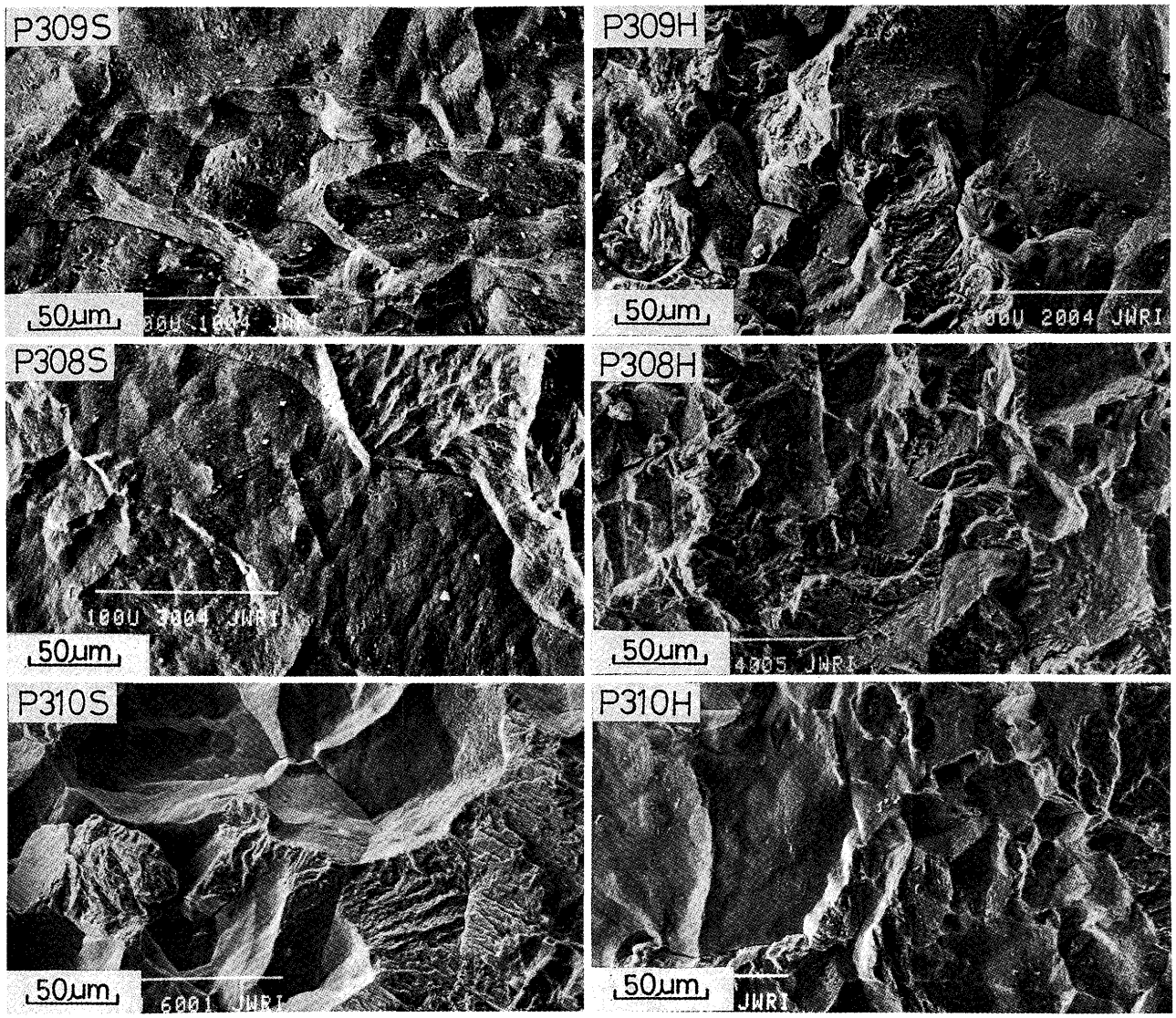

Photo. 4 Typical examples of fracture surface

Photograph 4 shows typical examples of fracture surface. In the case of P309S and P308S of high disbonding ratio, intergranular fracture surface was dominant. In the case of P309H and P308H of somewhat lower disbonding ratio, transgranular fracture surface increased a little. There seemed little difference in amounts of carbide precipitates on the fracture surface among these materials.

Also the fracture surface of P310S and P310H was intergranular, and the angle between adjacent intergranular facets was low, which was maybe caused by the characteristic of grain boundary formation. There was relatively little precipitates on the fracture surface.

As for the relation between the microstructure of overlaid metal and disbonding, it is shown[1] that duplex structure of austenite and martensite is less susceptible to cracking than only austenite and austenite with a few ferrite. The material P309H and P308H containing considerable amount of martensite surely showed relatively low disbonding ratio, but not completely zero. As one of the reason of this difference, non uniform distribution of martensite region as seen in **photo. 5** may be appointed. Photo. 5 includes the result of microhardness and X-ray counts of Ni and Cr Kα analyzed by EDX, and suggests that the austenite region contained relatively higher Ni and the martensite region contained relatively lower Ni, the tendency of which is supported by Schaeffler diagram. Such a change in microstructure was observed very often in P309H and P308H and this maybe caused by fluctuation of liquid flow under high speed-high current welding condition. In addition, this means that microstructure near the weld bond can not be explained by only average composition estimated by dilution ratio.

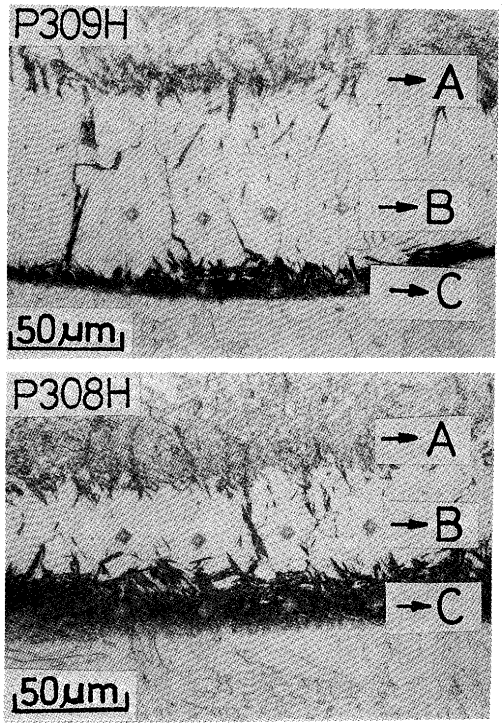

Location	Hardness* (Hv)	E.D.X.** analysis value	
		Cr (count)	Ni (count)
A	401	1261	226
B	285	1230	254
C	339	1044	178
Base metal	–	364	65

Location	Hardness* (Hv)	E.D.X.** analysis value	
		Cr (count)	Ni (count)
A	401	1195	223
B	285	1242	245
C	348	990	174
Base metal	–	380	68

* Load:10gf
** Total count:10000

Photo. 5 Nonuniform distributions of microstructure, hardness and composition near weld bond in P309H and P308H

3.2.2 Relation between width of carbide layer and location of disbonding

Figure 6 shows tipical example of hardness distribution near the weld bond. **Table 7** summarizes peak hardness and distance of the location showing the peak hardness from weld bond.

In the case of PWHT material, peak hardness generally occurred near the front edge of carbide layer, but in the martensite region as shown in Photo. 5 in P308H and P309H. In IncoS and IncoH, where carbide layer was very narrow, clear peak was not seen even in load of 10gf. Also in P309BS where buttering of low carbon 2 1/4Cr-1Mo martial was done, the hardness was not high.

Figure 7 show the relation between the distance distribution of disbonding from the weld bond and width distribution of carbide layer measured by the method shown in Fig. 2. Concerning the materials by standard welding condition, most frequent disbonding location is clearly seen, the distance of which become far in the order of P310S, P309S and P308S. This well agrees with the width distribution of carbide layer, and moreover nearly agrees with the hardness distribution in Fig. 6. On the other

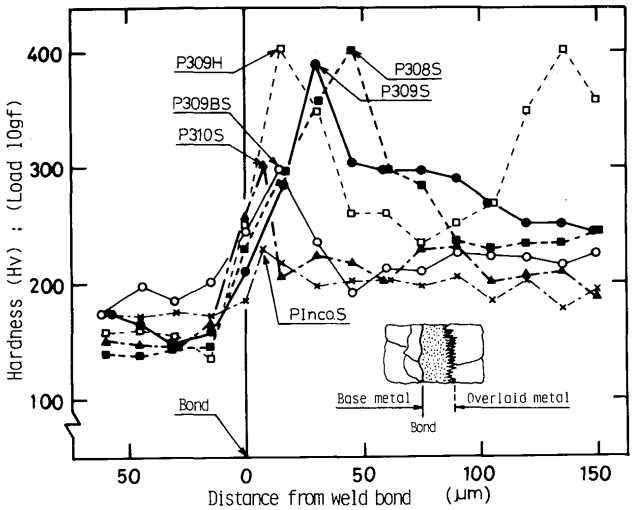

Fig. 6 Typical examples of hardness distribution near the weld bond

Table 7 Peak hardness and its distance from weld bond.

Material	Peak hardness (Hv)		Distance from bond	
	As-weld	PWHT	As-weld	PWHT
309S	378	389	3 0	3 0
309H	389	401	1 5	5,135
308S	378	401	2 5	4 5
308H	389	413	1 5	15,90
310S	330	301	0	5
310H	378	348	0	1 0
IncoS	330	229	0	5
IncoH	339	260	0	5
430S	413	339	1 0	3 0
309BS	339	297	3 0	1 5

hand, concerning the materials by high current and high speed welding condition, such a clear distribution is not seen except for P310S. Rather two frequent disbonding locations are seen in P309H and P308H. It is interesting that also such a complexed distribution nearly agrees with the width distribution of carbide layer. One of the reason for this complexed microstructure maybe attributed to the complexed microstructure as seen in photo. 5. All the results in Fig. 7 imply that the occurrence of disbonding is connected closely with carbide layer or hardened layer through some microstructural effects and accumulation and/or trapping effects of hydrogen around this layer.

4. Conclusions

Applicability of simulation test for disbonding by means of electrolytic hydrogen charging technique was

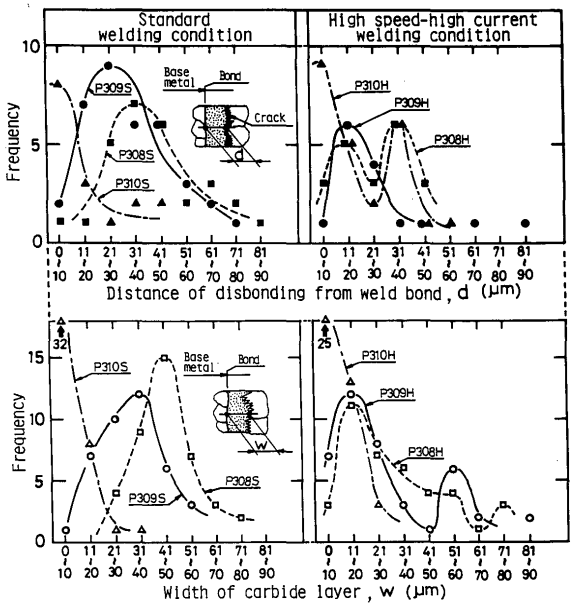

Fig. 7 Relation between distance distribution of disbonding from the weld bond and width distribution of carbide layer

studied. Main conclusions obtained are as follows:

1) Electrolytic hydrogen charging technique under suitable conditions can be utilized for the purpose of comparative test of disbonding susceptibility instead of autoclave method.
2) The suitable condition are: Specimen is nearly cube of each about 10 mm side which contains base metal of 2 mm thickness. Hydrogen is charged from the surface of base metal with no loading. The charging conditions are current density of $0.2A/cm^2$ and charging time of 24hr. The results by the condition well agree with those by severe condition in autoclave.
3) Disbonding easily occurred in PWHT materials overlaid with Type 309, 308, 310. No disbonding occurred in materials overlaid with Inconel or Type 309 combined with low carbon 2 1/4Cr-1Mo buttered metal. Disbonding occurred even in ferritic overlaid metal under very severe charging condition.
4) Microscopic ovservation showed that the disbonding mainly occurred at the front edge of hardened carbide layer. Therefore the buttering of low carbon 2 1/4Cr-1Mo steel prior to Type 309 overlaying was effective to prevent the disbonding.
5) High current and high speed welding of Type 309 and 308 decreased the disbonding ratio to some extent, but increased the ratio in Type 310. It seemed that complexed distribution of the hardened layer in the case of high current-high speed welding of Type 309 and 308 effects the occurrence of disbonding.

References

1) K. Naitoh, et al: JHPI, Vol. 18 (1980), No. 5, p. 263 (in

Japanese).

2) E. Takahashi, et al: WM-869-82 (Committee of welding metallurgy in Japan Welding Society).

3) K. Yasuda, et al: WM-891-82 (Committee of welding metallurgy in Japan Welding Society).

4) F. Matsuda, et al: Trans. JWRI, Vol. 13 (1984), No. 1, p. 159.

5) T. Ohmae, et al: WM-974-84 (Committee of welding metallurgy in Japan Welding Society).